Air Fraction Correction in PET Imaging of Lung Disease – Kernel Determination

Francesca Leek, *Student Member, IEEE*, Andrew P. Robinson, Robert M. Moss, Frederick J. Wilson, Brian F. Hutton, *Senior Member, IEEE*, and Kris Thielemans, *Senior Member, IEEE*

***Abstract*–Accurate quantification of radiotracer uptake from lung PET/CT is challenging due to large variations in fractions of tissue, air, blood, and water. The air fraction correction (AFC) determines voxel-wise air fractions (AF) from the CT acquired for attenuation correction (AC) to correct for the variable air content. However, the resolution mismatch between PET and CT can cause artefacts in the AF-corrected image. In this work, we compare different methodologies for determining the optimal kernel to smooth the CT for AFC, when PET images were reconstructed with iterative reconstruction methods, and in the case where AF-corrected lungs exhibit uniform uptake. Noiseless simulations and non-TOF MLEM reconstructions were performed with STIR via SIRF using a digital test-object constructed from a CT scan of a patient with idiopathic pulmonary fibrosis. The optimal smoothing for AFC was determined via i) the point-source insertion-and-subtraction-method, h_{pts}; ii) artefact reduction in the AF-corrected volume-of-interest (VOI), h_{AFC}; iii) smoothing a ground-truth image to match the reconstructed image within the VOI, h_{PVC}. Each of the three kernels were used to smooth the mu-map for AFC of the reconstructed emission data and the RMSE of each of the AF-corrected VOIs, with respect to the ground-truth, was assessed. Applicability of the preferred method was assessed with phantom acquisitions on a clinical scanner. Results demonstrated that, for iterative reconstruction methods, image resolution is dependent on iteration number and VOI density/uptake. Smoothing by h_{pts} resulted in the least quantitatively accurate AF-corrected images at fewer than 40 iterations. For both h_{AFC} and h_{PVC}, RMSE in the AF-corrected IPF regions is fairly stable across iterations. h_{PVC} has the potential to be utilised for determining the appropriate kernel for AFC on clinical scanners for application to patient PET/CT lung scans.**

I. Introduction

AIR fraction correction (AFC) assumes the observed activity concentration to be the radiotracer distributed throughout tissue (parenchyma and blood), and a gas component, containing no activity [1]. The CT for attenuation correction (AC) is used to determine voxel-wise air fractions (AF); correcting for these provides an estimate of tracer uptake per gram of tissue. The CT image is used for both AC and AFC; however, the resolution difference between PET and CT can cause artefacts in the AF-corrected PET image. A preliminary study demonstrated that, when lung tissue uptake is uniform, the CT resolution should match the PET system for AC but approximate the reconstructed PET image resolution for AFC [2]. This study confirmed that for iterative reconstruction methods, resolution is dependent on iteration number and the location of the volume-of-interest (VOI). We compare different methods for localised kernel determination for AFC and investigate whether AFC can be reliably performed, particularly in low count regions. Applicability of the preferred method is assessed with phantom acquisitions on a clinical scanner.

II. Methods

A. Simulations

An attenuation (mu) test-object was constructed by substituting the lungs in a digital XCAT phantom [3] with a diagnostic CT from an IPF patient, Fig. 1. The emission was simulated to produce a homogeneous AFCSUV = 1 in the lungs.

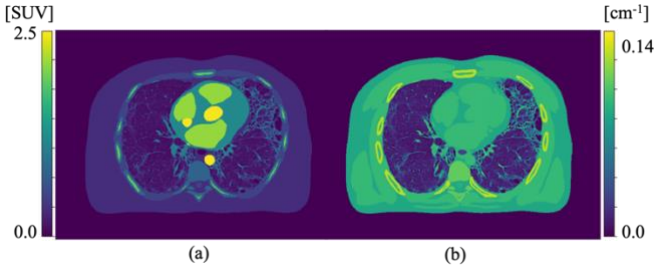

Fig. 1. Modified digital XCAT phantom (voxel size = 0.61 x 0.61 x 1.5 mm^3); (a) simulated emission; (b) simulated mu-map.

Data were simulated and reconstructed with a GE D710 PET template using STIR [4] via SIRF [5]. Both the emission and mu-map were convolved with an isotropic Gaussian kernel with a 4.7 mm full-width-half-maximum (FWHM) prior to forward-projection, to approximate the intrinsic resolution of the GE D710 [6]. All data were noiseless.

Manuscript received December 9, 2022. This work was supported by an EPSRC Industrial CASE award (EP/T517628/1), the UK National Physical Laboratory (NPL) through the National Measurement System Programmes Unit of the UK's Department of Business, Energy and Industrial Strategy, GlaxoSmithKline (BIDS3000035300) and the University College London (UCL) EPSRC Centre for Doctoral Training in Intelligent, Integrated Imaging in Healthcare (i4health; EP/S021930/1). Software used in this project is developed with supported from EPSRC (EP/T026693/1).

F. Leek is with the Institute of Nuclear Medicine, UCL, London NW1 2BU, UK and NPL, Teddington, Middlesex, W11 0LW, UK (email: francesca.leek.09@ucl.ac.uk).

B.F. Hutton, K. Thielemans are with the Institute of Nuclear Medicine, UCL. K.T. is also with the Centre for Medical Image Computing, UCL.

A. P. Robinson is with NPL, Christie Medical Physics and Engineering, The Christie NHS Foundation Trust, UK, and Schuster Laboratory, School of Physics and Astronomy, the University of Manchester, UK.

R. M. Moss is with the Department of Medical Physics and Biomedical Engineering, UCL, Gower Street, London WC1E 6BT, UK.

F. J. Wilson was with GlaxoSmithKline Research & Development Limited, Gunnels Wood Road, Stevenage, Herts, SG1 2NY, UK

Non-time-of-flight (TOF) MLEM reconstruction with 2000 iterations (i) was performed in 2.71 x 2.71 x 3.27 mm^3 voxels. The mu-map was smoothed with a matching kernel to the simulated intrinsic resolution of the PET scanner for AC [2].

HUs scale linearly to linear attenuation coefficients (LACs) in the lung [7], thus the relationship between the fraction of tissue in each voxel, k_v, and lung density can be expressed as:

$$\mu_v = k_v\mu_t + (1 - k_v)\mu_a \quad (1)$$

where μ_v, μ_t and μ_a are the LACs for 511 keV photons in the mu-map voxel, tissue, and air, respectively [1]. The simulated mu-map is smoothed, down-sampled, and the reconstructed emission image is divided by k_v on a voxel-wise basis.

The optimal kernel with which to smooth the mu-map for AFC was determined in six regions (three in healthy lung (HL) tissue, and three in regions of idiopathic pulmonary fibrosis (IPF)) via the three methods:

h_{pts}: the point-source insertion-and-subtraction method using a single voxel point-source (reconstructed contrast < 0.1 [8]).

h_{AFC}: the mu-map was smoothed by kernels of varying width; h_{AFC} denotes the kernel that resulted in the most homogeneous (lowest coefficient of variation (CoV)) AF-corrected volume of interest (VOI).

h_{PVC}: the ground truth emission was smoothed by kernels of varying width; h_{PVC} represents the kernel that resulted in the lowest root-mean-square-error (RMSE) in the VOI, with respect to the reconstructed emission image, similar to Joshi et al. [9].

For both h_{AFC} and h_{PVC}, the CT was convolved with 3D Gaussian kernels of decoupled in-plane and axial resolutions, of increasing FWHM (3–12 mm, 0.1 mm increments) and then down-sampled to the PET voxel size. 20 mm diameter VOIs were centered over the point-sources for kernel determination.

Each of the kernels were used to smooth the mu-map for AFC of the reconstructed data and the RMSE of each of the AF-corrected VOIs, with respect to the ground-truth, was assessed.

B. PET/CT acquisitions

The h_{PVC} methodology was utilised to determine the optimal kernel for AFC on the Siemens Biograph Vision 600, using a commercially available thorax phantom (ECT/LUNG-SPINE/I). The activity concentrations were such that the AF-corrected right lung, which contained a fillable spherical insert, would be homogeneous. Three clinical reconstructions were considered, "TOF" (post-filter (PF) = 4.0 mm, voxel size = 3.3 x 3.3 x 3.0 mm^3), "TOF + PSF" (PF = all-pass, voxel size = 1.65 x 1.65 x 3.00 mm^3), and "EARL2" (PF = 3.5 mm, voxel size = 3.3 x 3.3 x 3.0 mm^3). All reconstructions conducted a CT based AC, with a manufacturer determined kernel, and were run to four iterations with five subsets. The ground truth emission was constructed from known activity concentrations and a segmented high-resolution CT (HRCT) of the phantom. Fig. 2.

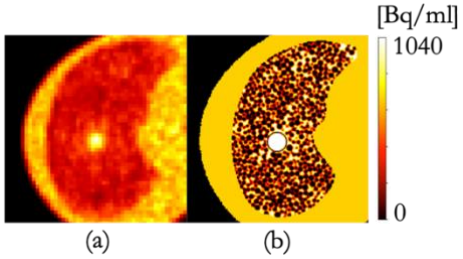

Fig. 2. Axial slice of (a) reconstructed PET thorax phantom; 4 ml spherical insert in the lung. Homogeneous AFC-Bq/ml = 1040 in lungs; (b) ground truth emission constructed from known activity concentration and segmented HRCT.

The optimal kernel for AFC was determined via h_{PVC} on a VOI positioned on the spherical insert.

III. Results

A. Simulations

Large numbers of iterations were needed to approach kernel width stability for each VOI. At 2000i MLEM, a large variation in estimated kernel FWHM still exists, depending on the position of the VOI and the method used to estimate it, Fig. 3(a). The lowest RMSE (0.06) was observed with h_{AFC} at 10i in the highest density/uptake IPF VOI. The highest RMSE (0.43) was observed in a HL VOI, at 10i, for h_{pts}, Fig. 3(b).

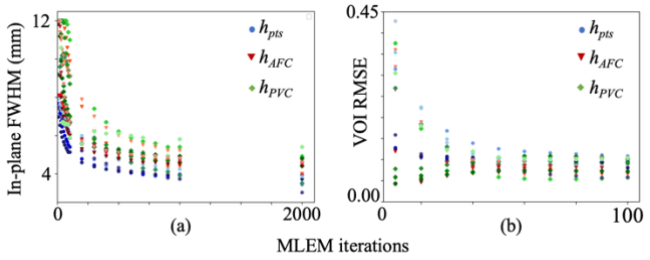

Fig. 3. (a) Estimated in-plane kernel width for AFC; (b) RMSE in VOI; both with respect to MLEM iteration number for each of the six VOIs, the lighter the marker, the lower the density/uptake the VOI; h_{pts}: blue, h_{AFC}: red, h_{PVC}: green.

h_{pts} resulted in the least accurate quantification for all AF-corrected VOIs at fewer than 40i. For both h_{AFC} and h_{PVC}, RMSE in the AF-corrected IPF regions is fairly stable across iterations.

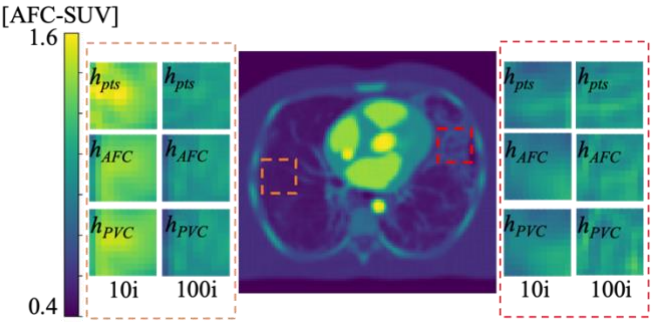

Fig. 4. (a) axial slice of reconstructed image at 1000 iterations flanked by AF-corrected regions surrounding HL VOI (orange) and IPF VOI (red); optimal kernels were used in each case; h_{pts}: top row; h_{AFC}: middle row; h_{PVC}: bottom row. Target AFC-SUV in the lung is 1.

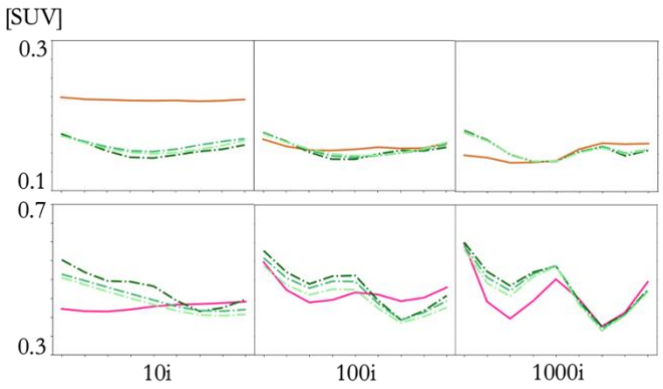

Fig. 5. Tangential profiles through reconstructed VOIs (top row: HL VOI, orange / bottom row: IPF VOI, magenta) and k_v-maps (green; h_{pts}: darkest, h_{AFC}: mid-; h_{PVC}: lightest).

B. PET/CT acquisitions

The minimum RMSE was ill-defined for all reconstructions investigated, Fig. 6. Increasing the number of iterations from 4 to 500 for the "TOF" reconstruction did not result in a more unique solution.

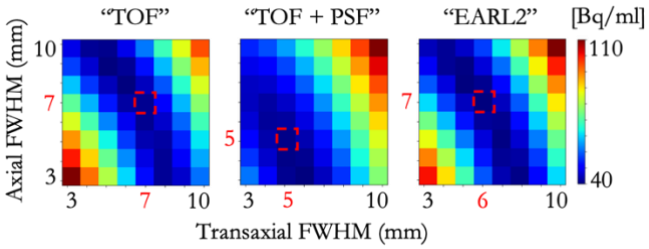

Fig. 6. Sphere VOI RMSE heatmap for AFC kernels for three clinical reconstructions. RMSE minima shown in red.

IV. Discussion and Conclusions

This study confirmed that for iterative reconstruction methods, reconstructed image resolution is dependent on iteration number and VOI density / uptake.

Fig. 3. shows that the three different methods obtain different resolution measures. h_{pts} resulted in the least accurate quantification for all AF-corrected VOIs at fewer than 40i. h_{pts} determines resolution based on small perturbations; at early iterations, the reconstruction is very non-linear, resulting in a mismatch between the resolution determined from the reconstructed perturbation, and that of the region to be corrected.

For both h_{AFC} and h_{PVC}, RMSE in the AF-corrected IPF regions is fairly stable across iterations. This indicates that the overall magnitude of uptake in these regions converges quickly, but the higher frequency detail of the highly heterogeneous structure of IPF, is not resolved until higher iterations.

h_{PVC} has the potential to determine the kernel for AFC for a clinical scanner; investigations into the difficulty in finding a unique solution are ongoing.

References

[1] T. Lambrou *et al.*, "The importance of correction for tissue fraction effects in lung PET: preliminary findings", Eur J Nucl Med Mol Imaging, 38:2238-2246, 2011.

[2] F. Leek, A.P. Robinson, R.M. Moss, F.J. Wilson, B.F. Hutton, K. Thielemans, "Air fraction correction optimisation in PET imaging of lung disease", 2020 IEEE NSS and MIC Conference Proceedings, 2020.

[3] W.P. Segars, G.Sturgeon, S. Mendonca, J. Grimes, B.M.W. Tsui, "4D XCAT phantom for multimodality imaging research", Med. Phys. 37(9):4902-4915, 2010.

[4] K. Thielemans *et al.*, "STIR: software for tomographic image reconstruction release 2", Phys Med Biol 57(4):867-883, 2012.

[5] E. Ovtchinnikov *et al.*, "SIRF: Synergistic Image Reconstruction Framework", Computer Phys Comms, 249:107087, 2020.

[6] V. Bettinardi, L. Presotto, E. Rapisarda, M. Picchio, L. Gianolli, M.C. Gilardi, "Physical performance of the new hybrid PET/CT Discovery-690", Med. Phys. 38(10):5394-5411, 2011.

[7] C. Burger, G. Goerres, S. Schoenes, A. Buck, A.H.R. Lonn, G.K. von Schulthess, "PET attenuation coefficients from CT images: experimental evaluation of the transformation of CT into PET 511-keV attenuation coefficients", Eur J Nucl Med 29:922-927, 2002

[8] K. Gong, S.R. Cherry, J. Qi, "On the assessment of spatial resolution of PET systems with iterative image reconstruction", Phys Med Biol, vol. 61, no. 5:193-202, 2016.

[9] A. Joshi, R.A. Koeppe, J.A. Fessler, "Reducing between scanner differences in multi-center PET studies", Neuroimage, 46(1):154-159, 2009.